NEUROSCIENCE

Forgetting generates a novel state that is reactivatable

He Liu[1,2]†‡, Taihong Wu[1,2]†, Xicotencatl Gracida Canales[1,2], Min Wu[1,2], Myung-Kyu Choi[1,2], Fengyun Duan[1,2], John A. Calarco[3], Yun Zhang[1,2]*

Forgetting is defined as a time-dependent decline of a memory. However, it is not clear whether forgetting reverses the learning process to return the brain to the naive state. Here, using the aversive olfactory learning of pathogenic bacteria in *C. elegans*, we show that forgetting generates a novel state of the nervous system that is distinct from the naive state or the learned state. A transient exposure to the training condition or training odorants reactivates this novel state to elicit the previously learned behavior. An AMPA receptor and a type II serotonin receptor act in the central neuron of the learning circuit to decrease and increase the speed to reach this novel state, respectively. Together, our study systematically characterizes forgetting and uncovers conserved mechanisms underlying the rate of forgetting.

INTRODUCTION

Forgetting is critical for the normal functions of the brain, which has a finite capacity (*1*–*3*). As described by Ebbinghaus's forgetting curve, forgetting is defined as a decline of memory over time. However, the nature of forgetting is not well understood. Behavioral studies on human subjects and animal models suggest that several factors contribute to forgetting, including natural decay whereby the neuronal correlates of memory dissipate over time and interference through which the information acquired after learning displaces previously formed memories (*1*–*3*). Psychophysics studies also suggest that forgetting, displayed as the weakening of a learned behavioral performance over time, could result from failed retrieval of the memories that continue to be encoded as experience-dependent changes of the brain. These findings suggest the possibility that forgetting does not erase the memory but renders it less accessible (*1*, *3*–*7*). We will not be able to fully address these questions and critically test these hypotheses on forgetting without directly examining the molecular correlates and neuronal activities of forgetting. Meanwhile, the rate of forgetting is integral to its function. Excessively persistent memories due to slow forgetting, especially those of aversive experience, may be associated with mental health issues in posttraumatic stress disorder (*8*). In addition, mutants of several autism-risk genes in *Drosophila* displayed reduced behavioral flexibility associated with impaired forgetting (*3*, *9*). Conversely, forgetting too fast undermines the function of learning. However, our current understanding of the underlying mechanism and the ability to manipulate the rate of forgetting is preliminary.

RESULTS

Caenorhabditis elegans forgets learned olfactory response over time

C. elegans adults form an aversive memory of the odorants of a pathogenic bacterium *Pseudomonas aeruginosa* strain PA14 (*10*)

after feeding on PA14 for 4 hours (*11*, *12*). *C. elegans* steers to attractive odorants and salts (*13*, *14*). We used an assay that measured the steering movement of individual animals to the odorants of PA14 to test learning immediately after training and to assess memory retention at different time points after returning the trained animals to the pretraining condition (Fig. 1, A and B, and Materials and Methods). This paradigm resembles those used to characterize forgetting when there is no evident interference. We used a navigation index that was defined as the ratio of radial speed (V_R) and the locomotory speed (V_L) and the traveling distance between the starting position and the end position to quantify the preference for the PA14 odorants (Fig. 1B, fig. S1, and Materials and Methods). A navigation index of 1 indicates the strongest preference measured in this assay (*14*). Compared with naive animals that were cultivated under standard conditions and fed on the benign bacterium strain *Escherichia coli* OP50 during training, worms trained by feeding on PA14 for 4 hours displayed a decreased navigation index and a longer traveling distance when tested immediately after training (Fig. 1, C to H), which indicates that the worms learned to reduce their preference for the odorants of PA14 and formed an aversive memory of the odorants. After 4 hours of training, some of the trained animals were moved to a plate containing *E. coli* OP50 and their aversive memory was measured at different time points afterward. We found that at 0.5 hours after training, the navigation index and the traveling distance were still comparable to those in trained animals, suggesting that the aversive memory was not yet forgotten (Fig. 1, C and D). At 1 hour after training, the navigation index and the traveling distance became comparable with those in naive animals and different from those in trained animals (Fig. 1, E and F) and exhibited no further change 2 hours after training (Fig. 1, G and H). Thus, it takes 1 hour for trained worms to forget the PA14-induced aversive memory under our experimental conditions. In addition, we found that the navigation index and the traveling distance when steering to the odorants of *E. coli* OP50 were similar in naive animals, PA14-trained animals, and animals that returned to the pretraining condition for 1 hour after training (Fig. 1, I and J), indicating the specificity of training and forgetting. Thus, we trained animals for 4 hours and used 1 hour after training as a time point to analyze forgetting in this study, unless otherwise specified.

The aversive memory can be rapidly reactivated after forgetting

Previous psychophysics studies showed that sensory cues associated with a previous learning experience could remind an animal of the

[1]Department of Organismic and Evolutionary Biology, Harvard University, Cambridge, MA 02138, USA. [2]Center for Brain Science, Harvard University, Cambridge, MA 02138, USA. [3]Department of Cell and Systems Biology, University of Toronto, Toronto, Ontario M5S 3G5, Canada.
*Corresponding author. Email: yzhang@oeb.harvard.edu
†These authors equally contributed to this work as co-first authors.
‡Present address: Advanced Institute of Natural Sciences, Beijing Normal University at Zhuhai, No.18, Jinfeng Road, Zhuhai, Guangdong, China.
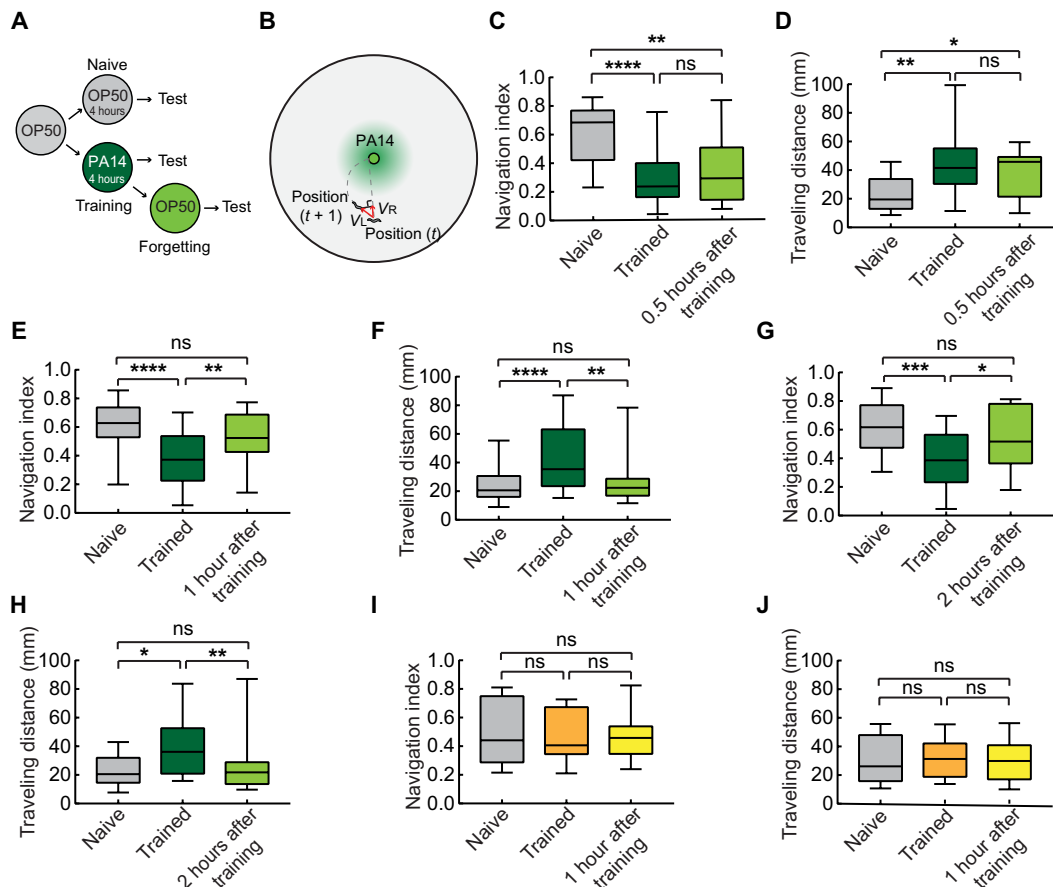
Fig. 1. _C. elegans_ forgets learned olfactory response over time. (**A** and **B**) Schematics of training (A) and testing (B) conditions for aversive olfactory learning and forgetting (Materials and Methods). V_R, radial speed; V_L, locomotory speed. (**C** to **H**) Animals trained with PA14 for 4 hours display decreased navigation indexes and increased traveling distance (C to H) when steering toward PA14 odorants; after returning to naive condition for 1 hour [(E and F) naive, $n = 35$; trained, $n = 38$; 1 hour after training, $n = 34$ animals], but not for 0.5 hours [(C and D) naive, $n = 17$; trained, $n = 18$; 0.5 hours after training, $n = 15$ animals], trained animals display navigation indexes and traveling distance comparable to naive ones. Forgetting for 2 hours does not further change navigation index or traveling distance [(G and H) naive, $n = 24$; trained, $n = 25$; 2 hours after training, $n = 28$ animals]. (**I** and **J**) Training with PA14 does not alter navigation index or traveling distance for chemotactic steering toward OP50 odorants either after training or after forgetting (naive, $n = 17$; trained, $n = 19$; 1 hour after training, $n = 18$ animals). For (C to J), one-way analysis of variance (ANOVA) with Tukey's multiple comparisons test (C, D, I, and J) or Kruskal-Wallis test with Dunn's multiple comparisons test (E to H); asterisks indicate significant difference, *$P < 0.05$, **$P < 0.01$, ***$P < 0.001$, and ****$P < 0.0001$; ns, not significant. Box plot, median and quartiles; whiskers, data range (minimum to maximum). P values are in data S6.

forgotten memory, which suggests that forgetting renders memory less accessible instead of erasing the memory (_1_, _3–7_). To examine whether the aversive memory of PA14 odorants was erased during forgetting, we reminded the worms after the 1-hour forgetting process by exposing them to a fresh culture of PA14 or the supernatant of the PA14 culture for only 3 min and subsequently tested their response to the PA14 odorants. Although it takes 4 hours for adult worms to complete the aversive learning of PA14 odorants (_11_), we found that 3-min exposure to a PA14 culture or the culture supernatant reactivated the aversive memory after forgetting and that the reactivated worms steered toward PA14 odorants with a significantly reduced navigation index and increased traveling distance compared with the worms that forgot (Fig. 2, A to D).

We further characterized memory reactivation using a previously established automated olfactory assay (_11_, _15_). In this assay, the bacterial odorants are delivered with air streams to worms that swim in droplets of buffer in an enclosed chamber, and the preference between the tested odorants were quantified by measuring the turning rate of the worms. We stimulated the worms with alternating

pulses of PA14 odorants and OP50 odorants and used a learning index to measure the difference between the preference of a tested animal and the average preference of the naive animals examined in parallel. A positive learning index indicated a learned avoidance of PA14 odorants (Materials and Methods) (_11_). We found that during the first half of the assay, animals trained with PA14 for 4 hours displayed the aversive learning of PA14 odorants and the animals that forgot showed learning indexes comparable to those generated by naive animals. However, after 5 cycles of exposure to PA14 odorants and OP50 odorants, the aversive memory in animals that forgot was reactivated, and these worms displayed learning indexes that were significantly higher than those in naive animals and comparable to those in trained animals (Fig. 2E and fig. S2). Thus, a transient exposure to PA14 odorants reactivates the aversive olfactory memory of PA14 after forgetting. Together, our results from experiments using three different ways to reactivate the aversive olfactory memory of PA14 show that after forgetting, the aversive memory is still encoded in the nervous system, which can be reactivated by transient exposure to the training condition or the odorants
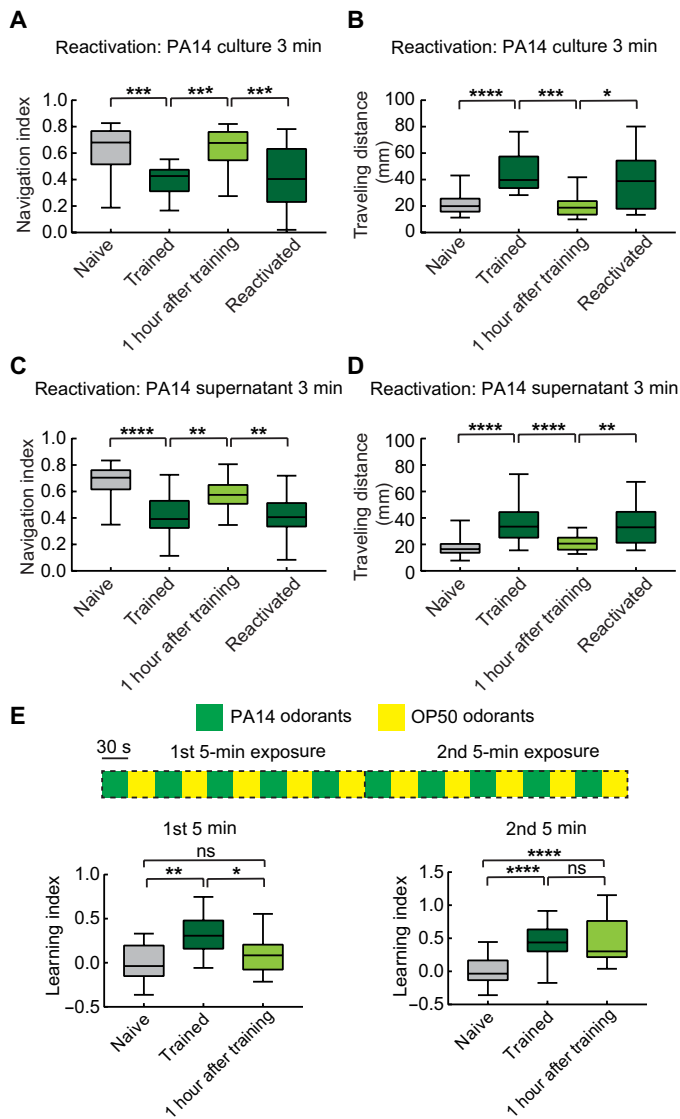
Fig. 2. Aversive memory can be rapidly reactivated after forgetting. (**A** to **D**) Training with PA14 decreases olfactory preference for PA14 odorants, which is forgotten after 1 hour; 3-min exposure to PA14 culture [(A and B) naive, $n = 20$; trained, $n = 18$; forgetting, $n = 18$; reactivation, $n = 16$ animals] or to PA14 culture supernatant [(C and D) naive, $n = 35$; trained, $n = 33$; forgetting, $n = 28$; reactivation, $n = 27$ animals] reactivates aversive memory to generate learned chemotactic steering toward PA14 odorants (A to D). One-way ANOVA with Tukey's multiple comparisons test (A) or Kruskal-Wallis test with Dunn's multiple comparisons test (B to D). (**E**) Exposure to pulses of PA14 odorants alternated with OP50 odorants for 5 min reactivates aversive memory to generate learned behavioral response to PA14 odorants after forgetting. Odorant pulses are used to reactivate aversive memory and to stimulate behavioral responses. A positive learning index indicates a decreased preference for PA14 odorants compared with OP50 odorants (Materials and Methods; $n = 16$ animals each for naive, trained, and 1 hour after training). Repeated measures two-way ANOVA with Tukey's multiple comparisons test for naive, trained, and 1 hour after training. For all, asterisks indicate significant difference: $*P < 0.05$, $**P < 0.01$, $***P < 0.001$, and $****P < 0.0001$. Box plot, median and quartiles; whiskers, data range (minimum to maximum). P values are in data S6.

that the animals were trained to form a memory of. These findings reveal that forgetting produces a state of the nervous system that generates behavioral outputs differently from the state of the naive or the trained animals.

Forgetting modulates the activity of a learning circuit

Next, we probed forgetting by characterizing the neural circuit underlying learning. Previously, we showed that a pair of interneurons RIA played a critical role in regulating aversive olfactory learning by mediating sensorimotor integration during odorant-guided steering movements (fig. S3) (*14*, *16*). The single process of RIA contains three functional domains: the proximal loop domain that receives sensory inputs and the distal nrV (nerve ring ventral) and nrD (nerve ring dorsal) domains that contain reciprocal synaptic connections with head motor neurons. The nrV and nrD domains generate compartmental activities, revealed by in vivo calcium imaging, that encode head bending information and inhibit head bending. Meanwhile, the loop domain receives sensory signals, such as those generated by PA14 odorants, to produce synchronized calcium responses in loop, nrV and nrD (*16*). The interaction between the sensory-evoked and the motor-encoding activities in nrV and nrD integrates the sensory and motor information to guide locomotory steering toward attractive odorants. Training with PA14 decreases the sensory-evoked synchronous activity in response to PA14 odorants and, thus, alters the outputs of nrV and nrD to reduce the efficiency of steering toward PA14, evidenced by a decreased navigation index and an increased traveling distance in trained animals (fig. S3) (*14*). Thus, we analyzed the activity of nrV and nrD domains to address the effect of forgetting on RIA activity patterns.

To examine how forgetting regulates RIA activity, we performed in vivo calcium imaging in a microfluidic system (*17*) using transgenic animals that expressed GCaMP3 (*18*) selectively in RIA (*16*). We stimulated animals with 1-s pulses of PA14 odorants at 0.5 Hz. In naive and trained animals and animals that forgot, nrV and nrD responded to PA14 pulses with 0.5-Hz synchronous calcium transients (Fig. 3, A to C), which generated a peak at 0.5 Hz after Fourier transform (Fig. 3, D to G). Consistent with our previous findings (*14*), the PA14-evoked synchronous response decreased in trained animals tested immediately after training compared with that in naive animals, which recovered at 1 hour after training (Fig. 3, A to G), consistent with the behavioral responses to PA14 odorants after training and after forgetting. In comparison, the calcium responses to 1-s pulses of OP50 odorants were not altered either by training or forgetting (Fig. 3H). RIA receives olfactory information from a pair of upstream interneurons AIY (*19*) to generate the synchronous sensory response critical for steering movements toward attractive odorants (*14*). Previous work showed that AIY was important for the aversive olfactory learning of PA14 (*11*). Using in vivo calcium imaging, we found that AIY responded to the pulses of PA14 odorants and training decreased the response of AIY. However, the sensory-evoked response in AIY remained decreased and comparable to the trained response at 1 hour after training. While AIY activity in naive animals is different from that in trained animals, AIY activity after forgetting cannot be distinguished from either the naive or the trained activity, displaying a pattern in between (Fig. 3, I to O). Together, the results on AIY and RIA suggest that forgetting modulates the neural circuit underlying the aversive olfactory learning to generate an activity pattern intermediate of that of the naive and the trained animals.
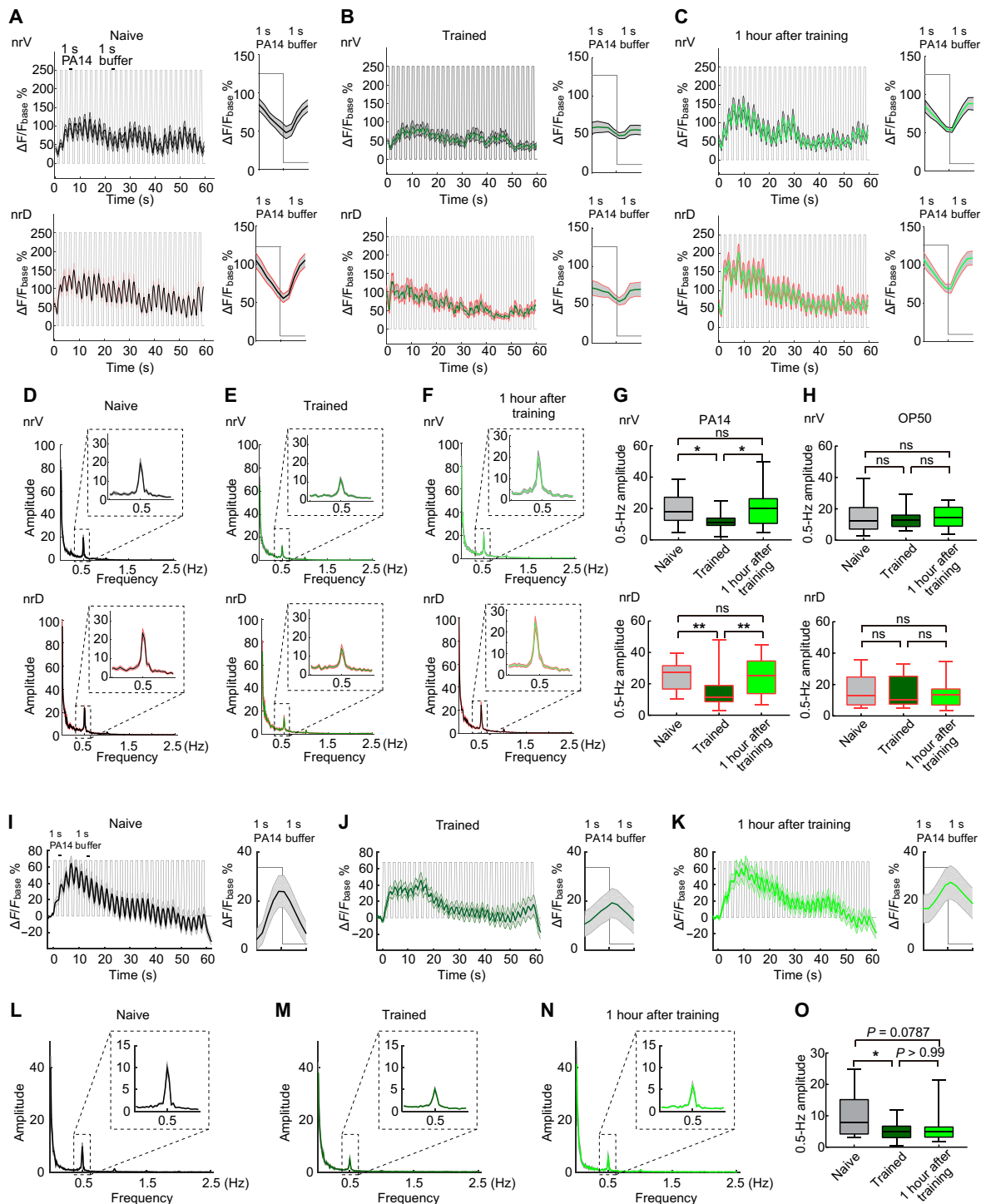
Fig. 3. Forgetting modulates neural circuit of olfactory learning. (A to **F)** Traces [(A to C), left] and average signals per stimulation cycle [(A to C), right] of GCaMP3 signals in nrV and nrD axonal domains of RIA evoked by pulses of PA14 odorants in naive animals [(A), $n = 18$], trained animals [(B), $n = 24$], and animals after forgetting [(C), $n = 20$] and respective Fourier transform of the GCaMP3 signals (D to F). (**G** and **H**) Amplitude of 0.5-Hz peak in Fourier transform of GCaMP3 signals of RIA nrV and nrD axonal domains evoked by pulses of PA14 odorants [(G) naive, $n = 18$; trained, $n = 24$; 1 hour after training, $n = 20$] or by pulses of OP50 odorants [(H) naive, $n = 15$; trained, $n = 15$; 1 hour after training, $n = 14$]. (**I** to **O**) Traces [(I to K), left] and average signals per stimulation cycle [(I to K), right] of GCaMP6 signals in AIY evoked by pulses of PA14 odorants in naive animals [(I), $n = 20$], trained animals [(J), $n = 21$], and animals after forgetting [(K), $n = 16$] and respective Fourier transform of the GCaMP6 signals (L to N) and amplitude of 0.5-Hz peak in Fourier transforms [(O) naive, $n = 20$; trained, $n = 21$; 1 hour after training, $n = 16$]. For (A to F and I to N), solid lines, mean; shades, SEM. $\Delta F = F - F_{base}$; for RIA, F_{base}, average intensity of bottom 5% fluorescence signals for each recording; for AIY, F_{base}, average intensity of 2-s recording before stimulation (Materials and Methods). One-way ANOVA with Tukey's multiple comparisons test [nrV in (G and H)] or Kruskal-Wallis test with Dunn's multiple comparisons test [nrD in (G and H), and O], *$P < 0.05$ and **$P < 0.01$. Box plot, median and quartiles; whiskers, data range (minimum to maximum). P values are in data S6.

Forgetting generates a novel translatome of the nervous system

To further characterize the state of the nervous system after forgetting, we analyzed actively translated genes in the nervous system of the naive animals, trained animals, and animals after forgetting (Fig. 1A). We performed translating ribosome affinity purification (TRAP) (20) using a transgenic strain that expressed the ribosomal protein large subunit RPL10a tagged with GFP (green fluorescent protein) in the entire nervous system (21). We precipitated the ribosome proteins from the nervous system using an anti-GFP antibody and purified actively translated mRNAs from the ribosomes. We used massively parallel sequencing to sequence the cDNA libraries and generated translational profiles for naive and trained animals and animals that forgot (Materials and Methods). Previous studies using this transgenic strain validated our approach to identify genes expressed in the nervous system (21).

We found 932 genes that were differentially expressed in the nervous system under the naive, training and forgetting conditions [false discovery rate (FDR) < 0.1; data S1 to S4 and Materials and Methods]. Among these genes, 594 genes produced different levels of ribosome-associated mRNAs in the nervous system in naive versus trained animals (Fig. 4A). Previous studies identified genes that changed expression after feeding on PA14 for 4 or 8 hours by quantifying all mRNAs that were produced and accumulated in the whole worms (22). While our method characterized neuronal mRNAs being actively translated on the ribosomes at the time of purification, around 30% of the genes that were regulated by feeding on PA14 for 4 or 8 hours (22) also showed differential expression in naive animals and trained animals in our study (fig. S4), which further validates our approach. Furthermore, we found that 245 genes generated different levels of ribosome-associated mRNAs between training and forgetting conditions and 440 genes between naive and forgetting (Fig. 4A). Principal component analysis (PCA) showed that these differentially expressed genes were well separated under the naive, training, and forgetting conditions (Fig. 4B). Hierarchical clustering or Pearson correlation clustering based on the quantified levels of these differentially expressed genes indicate that the translatomes of forgetting animals and trained animals are close together, and the naive translatome is further away from both forgetting and trained translatomes compared with the forgetting versus the trained (Fig. 4, C and D), although the animals that have forgotten display olfactory steering behavior comparable to the naive animals (Fig. 1). These results further reveal forgetting as a novel state that is different from the naive state despite the comparable chemotactic steering behaviors under these two conditions. In addition, only 14% of the genes differentially expressed between naive and training conditions are also differentially expressed between training and forgetting (Fig. 4A). Together, these analyses demonstrate that different genes are engaged during forgetting versus learning processes.

To understand the biological processes that are engaged by the differentially expressed genes, we analyzed GO (Gene Ontology) terms (23, 24) and KEGG (Kyoto Encyclopedia of Genes and Genomes) pathways (25) that are enriched in these genes (data S5). We did not find enrichment of main functional categories of neuronal genes, including ion channels, G protein–coupled receptors and signaling pathways, and neurotransmission pathways [data S5 and (26)]. The GO term analysis identified the enrichment of innate immune response and defense response to Gram-negative bacterium among several biological processes, consistent with the training experience with the pathogenic bacterium PA14 (data S5). The KEGG analysis identified the enrichment of the pathways for glutathione metabolism, metabolism of xenobiotics by cytochrome P450, and drug metabolism–cytochrome P450 that included genes regulating glutathione metabolism in the 932 differentially expressed genes (Fig. 4E, data S5, and Materials and Methods). Glutathione is present at a high concentration in the brain and plays a critical role in neural protective functions (27). Recent studies revealed a critical role of glutathione in regulating glutamatergic neurotransmission (28, 29). Glutamate serves as a substrate for the glutathione biosynthetic enzymes (27). Release of glutamate through metabolic processing of glutathione generates a significant amount of intracellular glutamate in the central nervous system. Thus, manipulating the metabolism or biosynthesis of glutathione alters intracellular glutamate concentration, presynaptic release of glutamate, and postsynaptic glutamate neurotransmission via mechanisms that are not well understood (28, 29). Notably, eight genes encoding glutathione transferases in *C. elegans* that catalyze glutathione to R-S-glutathione, which is able to generate glutamate subsequently, and one gene encoding a glutathione peroxidase involved in glutathione metabolism (30) showed altered expression after training or forgetting (Fig. 4F and data S1 to S4). Although it is not feasible for us to measure intracellular glutamate concentration in worms, these findings prompted us to consider glutamate signaling in learning and forgetting. Overall, the neuronal translatomes under naive, training, and forgetting conditions reflect the changes resulting from learning and forgetting, as well as the response of the nervous system to the pathogenicity of the training bacterium. We currently cannot disentangle these two possibilities. Furthermore, the translatomes of the whole nervous system are more likely to identify genes that are widely expressed or strongly regulated by the training and/or forgetting conditions. Nevertheless, these analyses provide molecular characterization that further demonstrates that the nervous system after forgetting differs from the nervous systems of the naive and the trained animals.

An AMPA-type glutamate receptor decreases the rate of forgetting

Next, we sought the function of a *C. elegans* AMPA-type glutamate receptor subunit GLR-1 in forgetting for several reasons. The *C. elegans* genome contains 10 genes that encode the homologs of vertebrate ionotropic glutamate receptor subunits (*glr-1, 2, 3, 4, 5, 6, 7, 8*, and *nmr-1, 2*) (26, 31, 32). Among these genes, *glr-1* encodes a homolog of the mammalian AMPA receptor subunits GluA1 and GluA2 (31), which regulate multiple forms of neural plasticity (33–35). Several *glr-1*–expressing neurons have been shown to play critical roles in the aversive olfactory learning of pathogenic bacteria (11, 12, 31, 36). However, the loss-of-function (*lf*) *glr-1(n2461)* adult mutant animals intriguingly display a normal aversive olfactory learning of PA14 (12). Thus, we wondered whether *glr-1* played a role in forgetting. We found that after training with PA14 for 4 hours, the *glr-1(n2461)* mutant animals exhibited a decreased navigation index and an increased traveling distance when steering toward the odorants of PA14, displaying a learning ability similarly as wild-type animals (Fig. 5, A and B, fig. S5, A and B), consistent with previous findings (12). However, the *glr-1(lf)* mutants forgot significantly faster than wild type. At 0.5 hours after training, the trained *glr-1(lf)* mutants already displayed a navigation index significantly larger
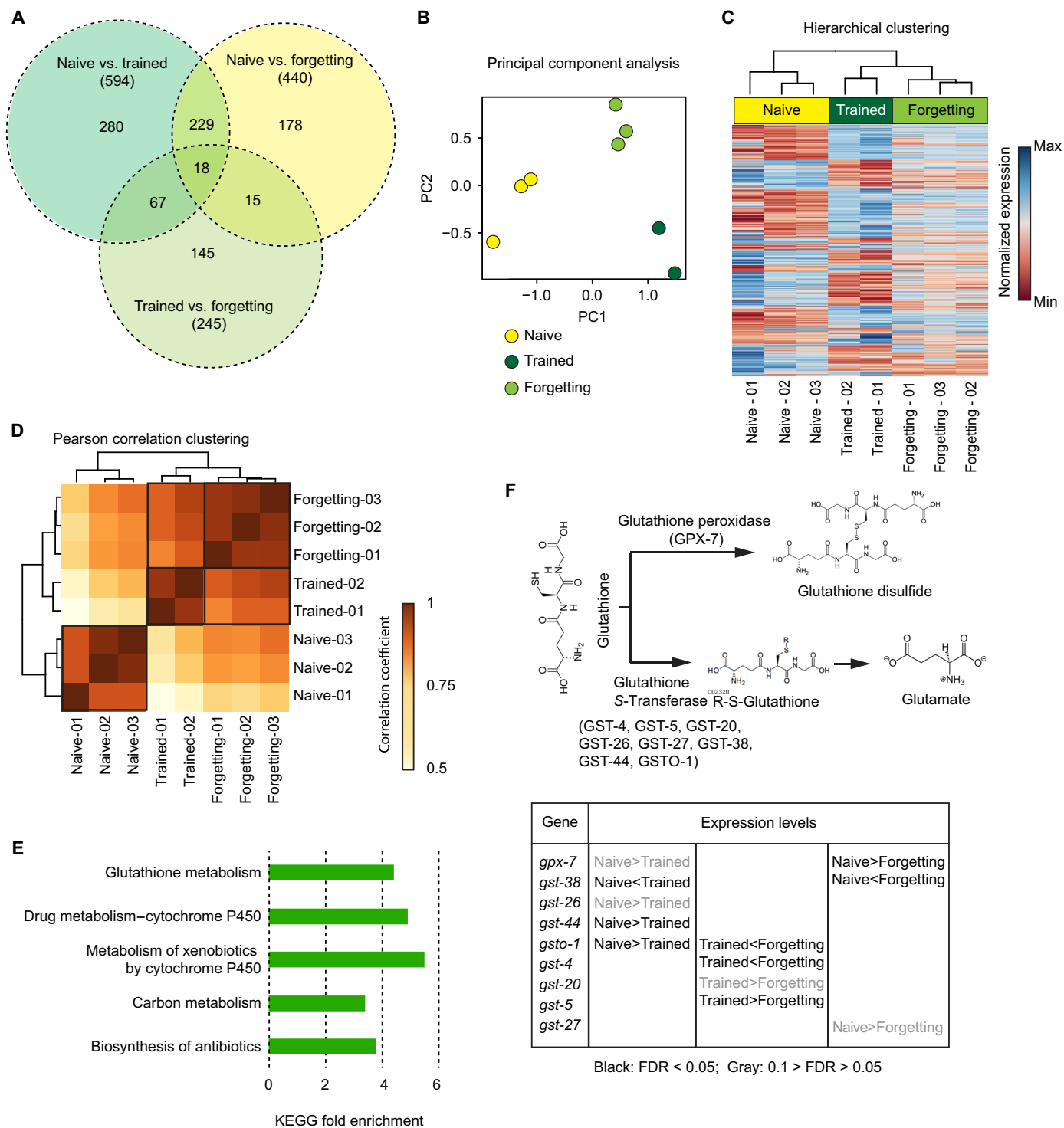
Fig. 4. Forgetting generates a novel translatome of the nervous system. (**A**) Venn diagrams showing genes differentially expressed in the nervous system under three conditions (naive, training, and forgetting, FDR < 0.1; data S1 to S4 and Materials and Methods). (**B** to **D**) Principal component analysis (B), hierarchical clustering (C) (each row represents one gene), and Pearson correlation clustering (D) based on the expression of genes differentially expressed in the nervous system under naive, training, and forgetting conditions (FDR < 0.1; Materials and Methods). (**E**) KEGG pathways enriched (FDR ≤ 0.05; data S5) in genes differentially expressed (data S1 to S4) in the nervous system under naive, training, and forgetting conditions (Materials and Methods). (**F**) Genes in glutathione metabolism pathways show differential expression under naive, training, and forgetting conditions. ">" and "<," respectively, denote higher or lower expression levels.
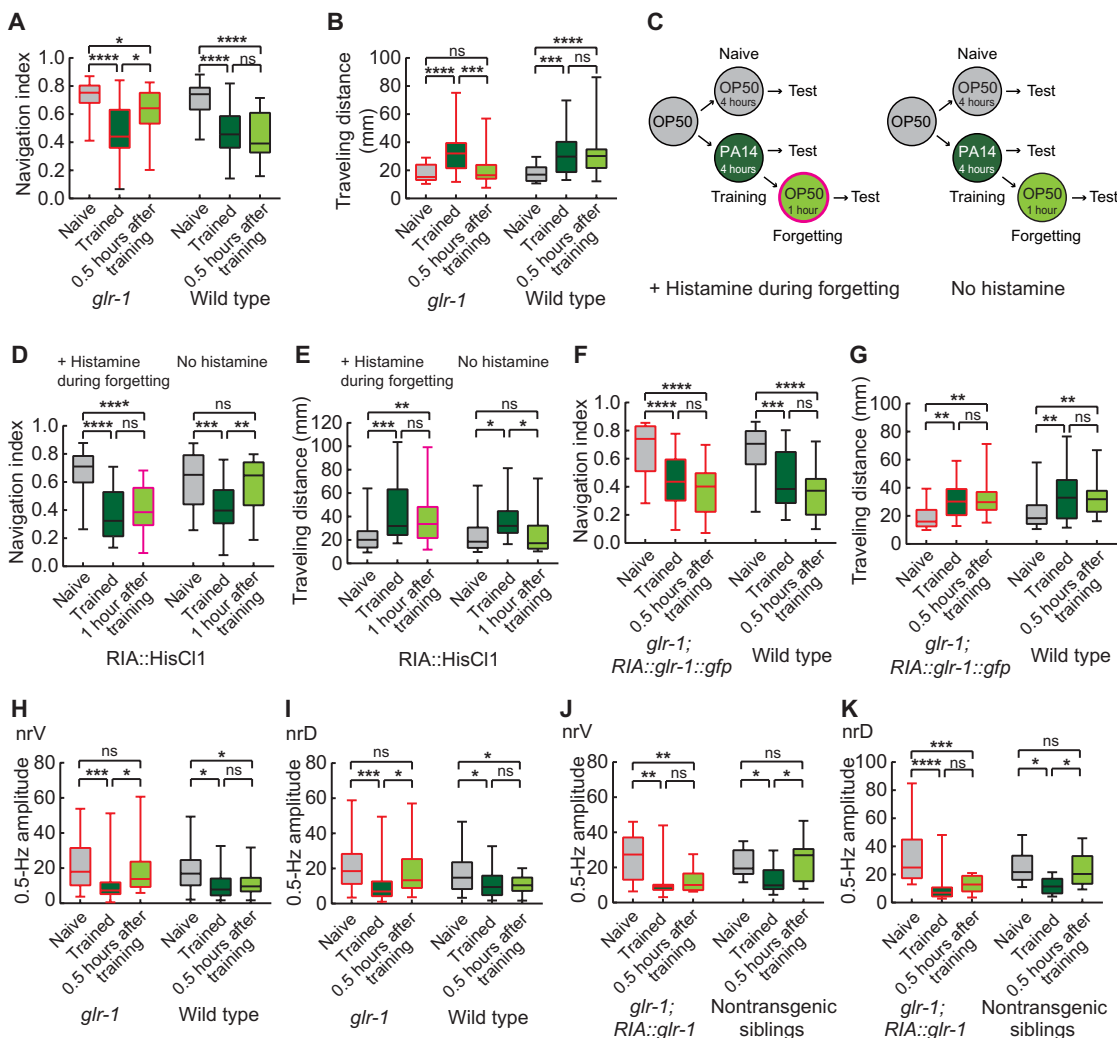
Fig. 5. AMPA-type glutamate receptor subunit GLR-1 acts in RIA to inhibit forgetting. (**A** and **B**) *glr-1(lf)* mutant animals display olfactory learning of PA14 but forget after 0.5 hour. *glr-1(lf)*: naive, *n* = 23; trained, *n* = 25; 0.5 hours after training, *n* = 23; wild type: naive, *n* = 29; trained, *n* = 29; 0.5 hours after training, *n* = 23 animals. (**C**) Schematics showing inhibition of RIA using histamine during forgetting. (**D** and **E**) Inhibiting RIA during forgetting by treating transgenic animals expressing HisCl1 in RIA with histamine blocks forgetting of PA14 memory (naive, *n* = 25; trained, *n* = 21; 1 hour after training, *n* = 28 animals); without histamine treatment, transgenic animals display olfactory learning and forgetting (naive, *n* = 24; trained, *n* = 24; 1 hour after training, *n* = 22 animals). (**F** and **G**) Expressing a wild-type *glr-1* gene in RIA rescues faster forgetting phenotype in *glr-1(lf)* mutants in olfactory steering to PA14. *glr-1;RIA::glr-1::gfp*: naive, *n* = 22; trained, *n* = 20; 0.5 hours after training, *n* = 20; wild type: naive, *n* = 24; trained, *n* = 20; 0.5 hours after training, *n* = 18 animals. (**H** to **K**) Amplitude of 0.5-Hz peak in Fourier transform of GCaMP3 signals of RIA axonal domains evoked by PA14 odorant pulses in *glr-1(lf)* mutants loses learning-dependent changes 0.5 hours after training [(H and I) *glr-1(lf)*: naive, *n* = 31; trained, *n* = 28; 0.5 hours after training, *n* = 29; wild type: naive, *n* = 32; trained, *n* = 29; 0.5 hours after training, *n* = 29 animals]; expressing a wild-type *glr-1* cDNA in RIA rescues [(J and K) *glr-1;RIA::glr-1*: naive, *n* = 12; trained, *n* = 12; 0.5 hours after training, *n* = 13; nontransgenic siblings: naive, *n* = 15; trained, *n* = 15; 0.5 hours after training, *n* = 13 animals]. For all, two-way ANOVA, Tukey's multiple comparisons test for naive, trained, and forgetting. Asterisks, significant difference; *$P < 0.05$, **$P < 0.01$, ***$P < 0.001$, and ****$P < 0.0001$. Box plot, median and quartiles; whiskers, data range (minimum to maximum). *P* values are in data S6.

than that generated immediately after training and a traveling distance significantly shorter than that generated immediately after training and comparable to that in naive animals, while the trained wild-type animals tested in parallel still exhibited the trained response to PA14 odorants (Fig. 5, A and B). These results together suggest that the AMPA-type glutamate receptor subunit GLR-1 slows down forgetting.

glr-1 is expressed in several neurons, including the interneurons RIA that regulate aversive olfactory learning of PA14 (*11*, *31*), and the GLR-1 protein is enriched in the process of RIA (*37*). Thus, we hypothesized that GLR-1 acted in RIA to regulate forgetting. To test

this mechanism, we first examined the role of RIA in forgetting by generating and testing transgenic animals that expressed a histamine-gated chloride channel subunit, HisCl1, in RIA using a cell-selective promoter *glr-3p* (*31*). Because *C. elegans* does not have an intrinsic ligand for histamine (*38*), treating the transgenic animals with histamine inducibly inhibits the activity of RIA. First, to test the function of the HisCl1 transgene in inhibiting RIA, we treated the transgenic animals with histamine at a standard concentration (10 mM) (*38*) immediately before and during chemotactic steering toward the odorants of PA14 (fig. S6A). We found that inhibiting RIA during steering significantly reduced the navigation index and

increased the traveling distance, consistent with the critical role of RIA in chemotactic steering as previously reported (fig. S6, B and C) (*14*). Next, to examine the role of RIA in forgetting, we inhibited RIA with histamine only during the forgetting process (Fig. 5C). Because we treated the worms with histamine for 1 hour during forgetting, we used a low concentration of histamine (~ 0.14 mM). We let the treated worms crawl on a plate with no histamine for 1 min before the assay and tested the chemotactic steering without the presence of histamine. To examine whether this treatment generally disrupted steering, we tested the treated animals for their chemotactic steering toward OP50 odorants because training with PA14 and forgetting do not alter steering toward OP50 odorants (Fig. 1). We found that inhibiting RIA only during forgetting under this condition did not generally disrupt steering, indicated by the similar steering movements toward OP50 odorants displayed by the naive and trained transgenic animals and transgenic animals treated with histamine during forgetting (fig. S6, D and E). However, this treatment blocked the forgetting of the olfactory memory of PA14. We found that after training with PA14 for 4 hours, the transgenic animals expressing HisCl1 in RIA learned to reduce their preference for PA14 odorants, evidenced by their decreased navigation index and increased traveling distance when steering toward PA14 (Fig. 5, C to E). However, after 1-hour forgetting process with the histamine treatment, these transgenic animals continued to exhibit a navigation index and a traveling distance similar as those exhibited immediately after training (Fig. 5, C to E). As a control, the transgenic animals without the histamine treatment during forgetting forgot the learned olfactory response to PA14 after 1 hour (Fig. 5, C to E). These results together with our previous findings demonstrate that the RIA interneurons regulate learning and forgetting.

Next, we expressed a functional translational fusion GLR-1::GFP specifically in RIA (*37*) in the *glr-1(lf)* mutants and found that the RIA-selective expression of *glr-1* fully rescued the fast forgetting phenotype of the mutant animals, and at 0.5 hours after training, the rescued animals showed navigation indexes and traveling distance comparable to those generated immediately after training (Fig. 5, F and G). Using in vivo calcium imaging, we found that RIA calcium transients evoked by the pulses of PA14 odorants decreased after training in the *glr-1(lf)* mutants but increased back to the naive level only 0.5 hours after training, a time point when wild type still exhibited learning-induced decrease in PA14-evoked RIA calcium responses (Fig. 5, H and I). The faster recovery of RIA activity during forgetting in *glr-1(lf)* mutants is consistent with the faster forgetting of the mutants in behavior (Fig. 5, A and B). Similarly, expressing a wild-type *glr-1* cDNA in RIA rescued the defect of the *glr-1(lf)* mutant animals in PA14-evoked RIA calcium responses during forgetting (Fig. 5, J and K). At 0.5 hours after training, the rescued animals showed RIA calcium responses comparable to those generated immediately after training, while the nontransgenic siblings showed calcium responses comparable to the naive ones at 0.5 hours after training (Fig. 5, J and K). Together, these results show that GLR-1 acts in RIA to slow down forgetting.

A serotonin receptor SER-1/HTR2B acts in RIA to accelerate forgetting

Next, to address how GLR-1 slows down forgetting, we probed the role of serotonin signaling. Serotonin regulates hippocampal memory storage and learning speed in mice (*39*, *40*). In *C. elegans*, serotonin signaling regulates aversive olfactory learning of pathogenic bacteria

during the adult stage and in imprinting (*12*, *14*, *41*, *42*). The *C. elegans* genome encodes several serotonin receptors (*42–48*). We and others previously showed that a serotonin-gated chloride channel MOD-1 acted in the interneurons AIB/AIZ or AIY, and a serotonin-gated cation channel LGC-50 acted in RIA to regulate the aversive learning of PA14 (*12*, *14*, *41*, *42*). Another serotonin receptor, SER-1, is expressed in RIA (*32*, *44*, *45*). The SER-1 protein is enriched in the distal region of the RIA axon (*47*), where the sensory-evoked and motor-generated calcium signals integrate to direct motor outputs for olfactory steering (*14*). We found that training with PA14 decreased the navigation index and increased the traveling distance in *ser-1(ok345)* loss-of-function mutants, similarly as in wild type (fig. S5, C and D); however, different from wild-type animals, *ser-1(lf)* mutants continued to show the trained behavioral response to PA14 odorants at 1 hour after training (Fig. 6, A and B). While wild-type animals forget after returning to the pretraining condition for 1 hour, it took 4 hours for the *ser-1(lf)* mutants to forget (fig. S7), indicating that the *ser-1(lf)* mutants are slower in forgetting. Furthermore, we found that the sensory-evoked calcium transients in response to 1-s pulses of PA14 odorants decreased immediately after training in the *ser-1(lf)* mutants, similarly as in wild type, consistent with the normal learning behavior in the *ser-1(lf)* mutant animals. However, the PA14-evoked calcium signals in the *ser-1(lf)* mutant animals remained decreased at 1 hour after training (Fig. 6, C and D), consistent with the slower forgetting phenotype in behavior. Expressing a wild-type *ser-1* cDNA in RIA fully restored the normal forgetting process in behavior and in RIA calcium responses in the *ser-1(lf)* mutant animals (Fig. 6, E to H). These results together indicate that SER-1 acts in RIA to accelerate forgetting.

The opposite phenotypes of the *glr-1(lf)* and *ser-1(lf)* mutants prompted us to test the *glr-1(lf);ser-1(lf)* double mutant animals in forgetting. We found that training with PA14 induced the aversive olfactory learning in the double mutants (Fig. 7, A and B, and fig. S5, E and F); however, at 1 hour after training, the *glr-1(lf);ser-1(lf)* animals continued to display navigation indexes and traveling distance that were respectively smaller and longer than those produced under the naive condition and comparable to those produced immediately after training, showing a slower forgetting phenotype in behavior similar to the *ser-1(lf)* mutant animals (Fig. 7, A and B). Meanwhile, we found that training significantly suppressed the PA14-evoked calcium responses in RIA in the *glr-1(lf);ser-1(lf)* mutants, consistent with their normal learning behavior. However, at 1 hour after training, while RIA calcium responses in the wild-type controls were already different from those in trained animals, the RIA calcium responses in the double mutants could not be distinguished from either the trained responses or the naive responses, showing an intermediate phenotype (Fig. 7, C and D). Together, the results in behavior and RIA calcium responses suggest that either SER-1 acts downstream of GLR-1 to regulate forgetting rate with GLR-1 inhibiting forgetting by partly suppressing the function of SER-1 or GLR-1 and SER-1 regulate forgetting rate in an opposing manner in parallel pathways with SER-1 having a stronger effect.

To test these two possibilities and further address the function of GLR-1 and SER-1 in forgetting, we next examined the expression of GLR-1 and SER-1 in RIA. We first measured the expression of GLR-1 in RIA using a functional translational fusion GLR-1::GFP that was specifically expressed in RIA using a *glr-3* promoter and enriched in the proximal region of the RIA axon (*37*). We found that either training or forgetting did not significantly change the expression of
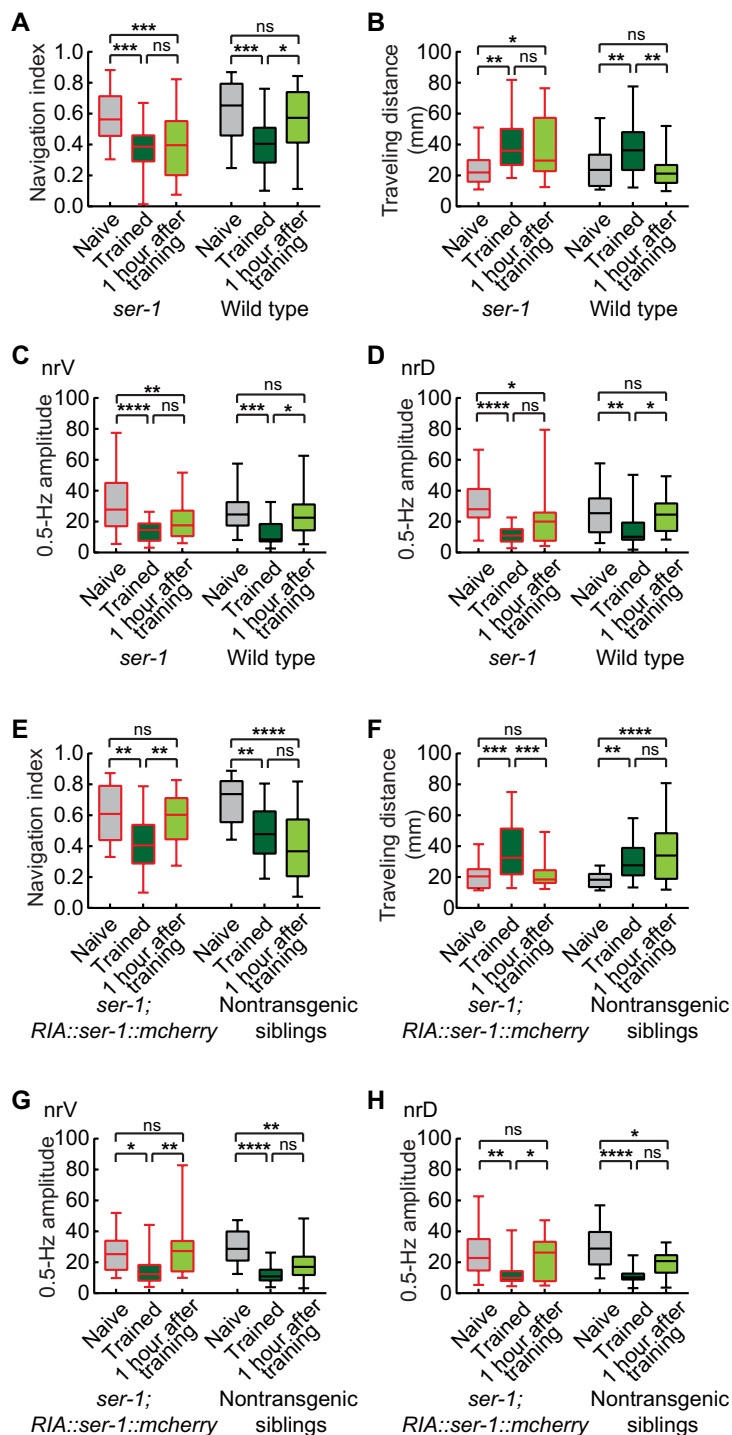
Fig. 6. SER-1, a homolog of HTR2B, acts in RIA to accelerate forgetting. (**A** and **B**) *ser-1(lf)* mutant animals learn to reduce preference for PA14 odorants but do not forget 1 hour after training. *ser-1(lf)*: naive, $n = 27$; trained, $n = 26$; 1 hour after training, $n = 26$ animals; wild type: naive, $n = 23$; trained, $n = 25$; 1 hour after training, $n = 21$ animals. (**C** and **D**) Amplitude of 0.5-Hz peak in Fourier transform of GCaMP3 signals of RIA nrV and nrD axonal domains evoked by pulses of PA14 odorants in *ser-1(lf)* mutants displays learning-dependent changes but maintains the changes 1 hour after training. *ser-1(lf)*: naive, $n = 28$; trained, $n = 20$; 1 hour after training, $n = 21$ animals; wild type: naive, $n = 24$; trained, $n = 23$; 1 hour after training, $n = 23$ animals. (**E** to **H**) Expressing a wild-type *ser-1* cDNA in RIA rescues slow forgetting phenotype in *ser-1(lf)* mutants in behavior [(E and F) *ser-1;RIA::ser-1::mCherry*: naive, $n = 21$; trained, $n = 21$; 1 hour after training, $n = 21$ animals; nontransgenic siblings: naive, $n = 22$; trained, $n = 22$; 1 hour after training, $n = 21$ animals] and in RIA neuronal activity [(G and H) *ser-1;RIA::ser-1::mCherry*: naive, $n = 18$; trained, $n = 15$; 1 hour after training, $n = 15$ animals; nontransgenic siblings: naive, $n = 23$; trained, $n = 16$; 1 hour after training, $n = 21$ animals]. For all, two-way ANOVA, Tukey's multiple comparisons test for naive, trained, and forgetting, Asterisks, significant difference; $*P < 0.05$, $**P < 0.01$, $***P < 0.001$, and $****P < 0.0001$. Box plot, median and quartiles; whiskers, data range (minimum to maximum). P values are in data S6.
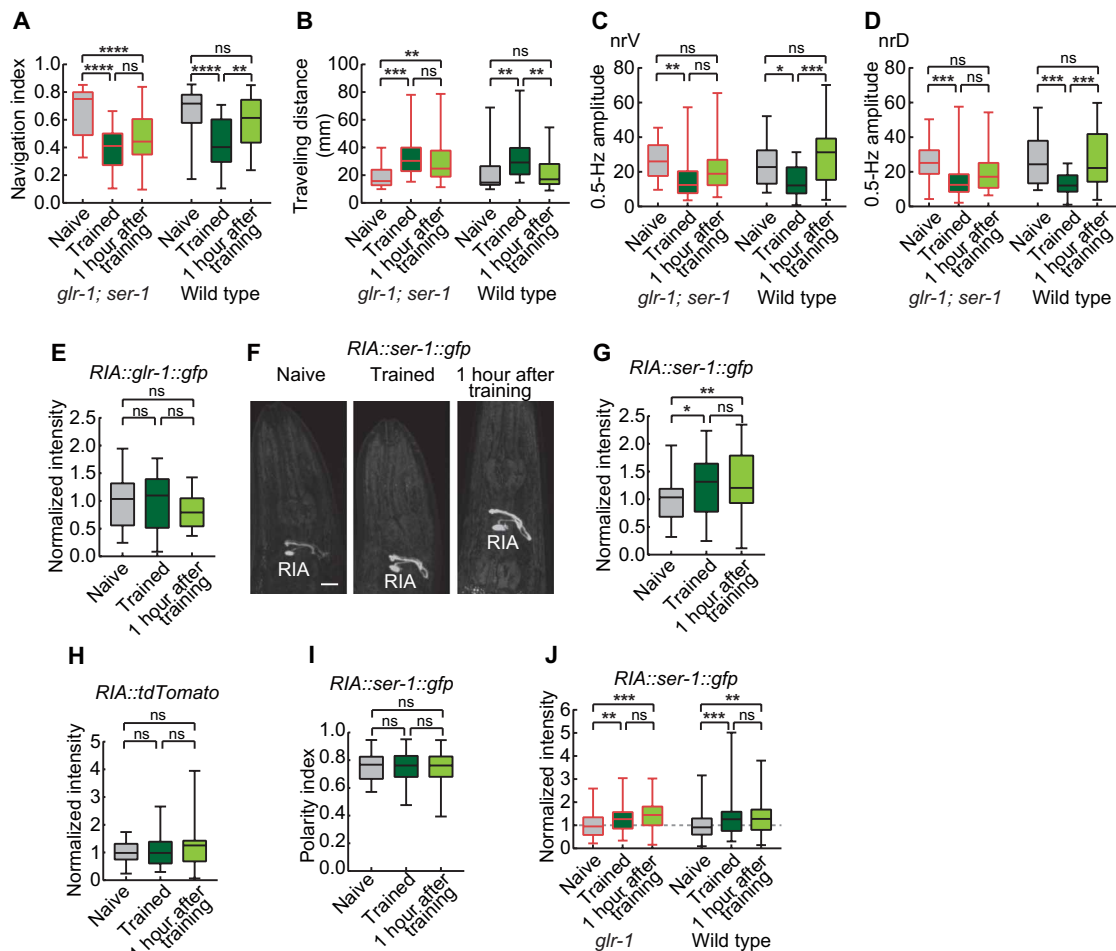
Fig. 7. GLR-1 and SER-1 regulate forgetting rate in parallel pathways. (**A** and **B**) *glr-1;ser-1* mutants display olfactory learning of PA14 but do not forget after 1 hour. *glr-1;ser-1*: naive, *n* = 33; trained, *n* = 27; 1 hour after training, *n* = 32; wild type: naive, *n* = 25; trained *n* = 29; 1 hour after training, *n* = 25. (**C** and **D**) Amplitude of 0.5-Hz peak in Fourier transform of GCaMP3 signals of RIA axonal domains evoked by PA14 odorant pulses in naive and trained *glr-1;ser-1* mutants, and 1 hour after training. *glr-1;ser-1*: naive, *n* = 38; trained, *n* = 24; 1 hour after training, *n* = 31; wild type: naive, *n* = 22; trained, *n* = 21; 1 hour after training, *n* = 21. (**E**) GLR-1::GFP level in RIA axon is not regulated by training or forgetting. Naive, *n* = 30; trained, *n* = 31; 1 hour after training, *n* = 34 animals. (**F**) Images of SER-1::GFP expressed using an RIA-specific promoter. Scale bar, 15 μm. Anterior, up; dorsal, left. (**G** to **I**) SER-1::GFP level in RIA distal axonal region increases after training and forgetting [(G) naive; *n* = 49; trained, *n* = 50; 1 hour after training, *n* = 49 animals]; training does not increase *glr-3p::tdTomato* expression in the same region [(H) *n* = 34 animals each] or change polarity of SER-1::GFP expression [(I) *n* = 20 animals each]. Polarity index indicates distribution of SER-1::GFP in RIA axon (Materials and Methods). (**J**) Training increases SER-1::GFP level in RIA in *glr-1(lf)* mutants. *glr-1(lf)*: naive, *n* = 86; trained, *n* = 95; 1 hour after training, *n* = 64; wild type: naive, *n* = 94; trained, *n* = 94; 1 hour after training, *n* = 71. Fluorescence intensity is normalized using average intensity of control naive animals (E, G, H, and J). One-way ANOVA with Tukey's multiple comparisons test (G and I), Kruskal-Wallis test with Dunn's multiple comparisons test (E and H), or two-way ANOVA with Tukey's multiple comparisons test for naive, trained, and forgetting (A to D and J); *P < 0.05, **P < 0.01, ***P < 0.001, and ****P < 0.0001. Box plot, median and quartiles; whiskers, data range (minimum to maximum). *P* values are in data S6.

GLR-1 in the RIA axon (Fig. 7E). Next, we measured the expression level of SER-1 in RIA using a functional translational fusion SER-1::GFP that was selectively expressed in RIA using a *glr-3* promoter (*47*). The SER-1::GFP fusion is enriched in the distal region of the RIA axon (*47*), and we found that training increased the level of SER-1::GFP in the distal axonal region and remained increased at 1 hour after training (*RIA::ser-1::gfp*; Fig. 7, F and G). A transcriptional reporter *Pglr-3::tdTomato*, as a control for the promoter activity, did not show any training-induced change in its expression in the same axonal region (*RIA::tdTomato*; Fig. 7H). In addition, the enrichment of SER-1::GFP in the distal region of RIA axon, measured by a polarity index, was not altered by training or forgetting (Fig. 7I and Materials and Methods). These results together indicate that training increases the abundance of SER-1 protein in RIA. To test whether GLR-1 regulates the training-induced

expression of SER-1, we measured the level of SER-1::GFP in RIA in the *glr-1(lf)* mutant animals and found that inactivating *glr-1* did not block the training-induced increase in the SER-1::GFP level immediately after training or after forgetting (*RIA::ser-1::gfp*; Fig. 7J). Together, these results show that training increases the level of SER-1, a type II serotonin receptor that accelerates forgetting and that the training-induced increase in SER-1 expression does not depend on GLR-1, supporting parallel pathways for GLR-1 and SER-1 to regulate forgetting rate in an opposing manner (Fig. 8).

DISCUSSION
Using a form of olfactory learning in *C. elegans*, we show at the molecular, cellular, and organismic levels that forgetting produces a
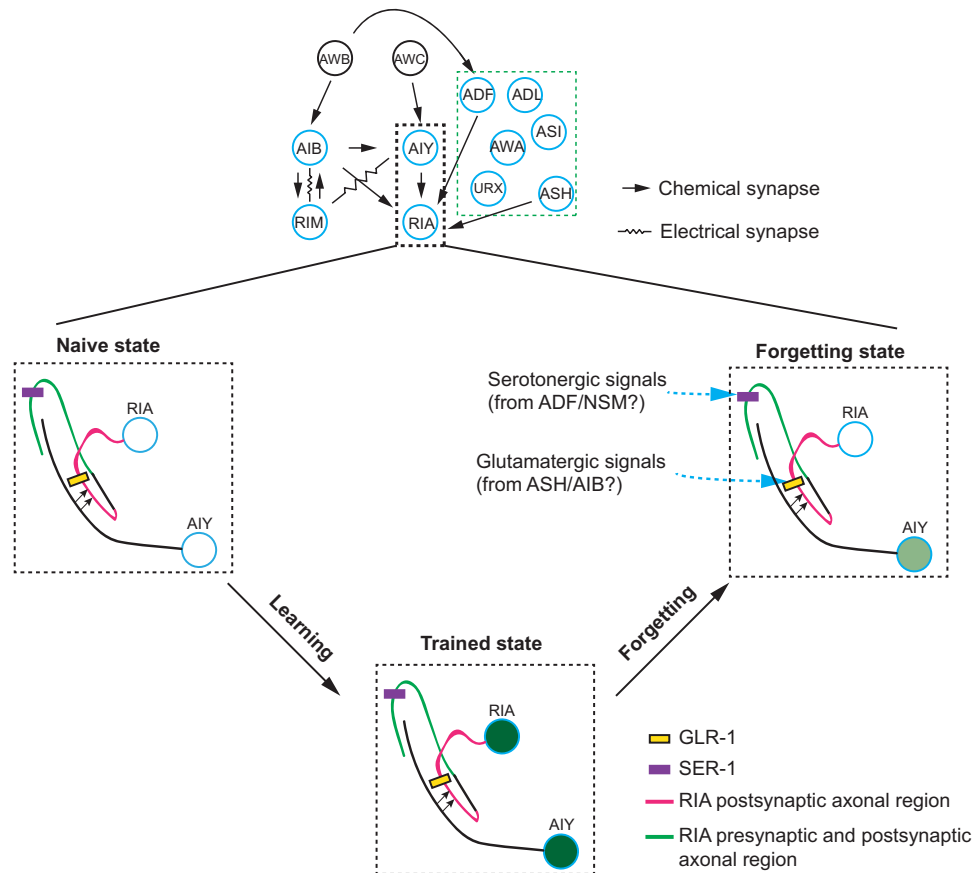
Fig. 8. A working model. Previously identified neurons that regulate olfactory learning of pathogenic bacterium PA14 in adult *C. elegans* (*11*, *12*, *36*, *41*, *49–51*) include interneurons AIY, RIA, AIB, and RIM, which receive synaptic inputs, directly or indirectly, from sensory neurons, such as olfactory neurons AWB and AWC. Sensory neurons ADF, ADL, ASI, ASH, AWA, and URX generate modulatory signals for learning. Training alters neuronal activities, including responses of AIY, RIA, AIB, and RIM to PA14 odorants, to encode memory [Fig. 3 and (*14*, *36*)]. After forgetting, learning-correlated changes are maintained in AIY but removed from RIA. RIA integrates olfactory sensory inputs and motor feedback to regulate sensorimotor responses (*14*, *16*, *19*) and receive synaptic inputs from AIY to generate PA14 odorant–evoked responses. Training with PA14 alters sensory responses of AIY and RIA, which reduces olfactory steering toward PA14 [Fig. 3 and (*14*)]. During forgetting, glutamatergic signals and serotonergic signals modulate RIA activity, respectively, via GLR-1 and SER-1 in RIA downstream of AIY, generating olfactory steering to PA14 similarly as naive animals. Serotonergic neurons ADF and NSM may provide modulatory signals for forgetting. Glutamatergic presynaptic neurons of RIA, including AIB and ASH (*55*), which generate learning-dependent changes (*36*), may provide glutamatergic inputs for forgetting. Overall, RIA integrates different neuronal inputs during learning versus forgetting to produce different levels of olfactory steering toward PA14. For simplicity, not all neurons implicated in aversive learning are shown and not all synapses are shown; thickness of the arrows or lines does not represent synapse numbers. Neuronal activity is measured from axons of RIA and AIY; cell bodies are highlighted for simplicity.

state of the nervous system that is distinct from the naive state and the trained state. In our study, we return the trained animals to the pretraining condition, a paradigm that examines forgetting when no evident interference is introduced. We show that although forgetting takes place in an environment identical to the naive condition, it does not reverse the learning process nor returns the nervous system to the naive status. On the basis of our results, we propose that forgetting engages specific functions of the nervous system to produce a new state. The new state allows the animals to rapidly display the previously learned behavior when they are reminded of the previous learning experience with transient exposure to the training condition or part of the training condition.

Previous studies using laser ablation, molecular genetics, and functional imaging approaches have identified neurons that regulate the aversive olfactory learning of the pathogenic bacterium PA14 in adult *C. elegans* (*11*, *12*, *36*, *41*, *49–51*). These include interneurons AIY, RIA, AIB, and RIM. These interneurons are connected through

chemical and electrical synapses and receive multiple synaptic inputs, directly or indirectly, from sensory neurons, including the main olfactory sensory neurons AWB and AWC. The sensory neurons ASI, AWA, ADL, and URX and the serotonergic neuron ADF generate modulatory signals important for memory formation (Fig. 8). Training alters the activity of the nervous system, including the responses of AIY, RIA, AIB, and RIM to the PA14 odorants, to encode the aversive olfactory memory [Fig. 3 and (*14*, *36*)]. Here, we show that after forgetting, the learning-correlated activity change is maintained in AIY but removed from RIA through the function of GLR-1 and SER-1 in RIA. RIA integrates multiple synaptic inputs, including olfactory sensory inputs and motor feedback, to generate sensorimotor responses (*14*, *16*, *19*). RIA receives synaptic inputs from the cholinergic interneuron AIY to generate PA14 odorant–evoked sensory responses (*14*). Training with PA14 alters the sensory responses of both AIY and RIA, which reduces olfactory preference toward PA14 during chemotactic steering [Fig. 3 and (*14*)]. During

forgetting, a glutamatergic signal and a serotonergic signal modulate the activity of RIA via the function of GLR-1 and SER-1 downstream of AIY, generating olfactory steering to PA14 similarly as naive animals (Fig. 8). Both serotonergic neurons ADF and NSM respond to bacterial food (*52–54*) to potentially provide a modulatory signal to regulate forgetting. Several presynaptic neurons of RIA are glutamatergic, including the interneuron AIB and the nociceptive sensory neuron ASH (*55*), both of which generate learning-dependent changes in their PA14-evoked responses (*36*). These neurons may provide glutamatergic inputs during forgetting to modulate RIA. Overall, RIA integrates different neuronal inputs during learning versus forgetting to produce different levels of olfactory steering toward PA14 (Fig. 8).

Several previous studies investigating the mechanism of forgetting identified important roles of dopamine signaling and pathways that regulate cytoskeleton remodeling (*56–59*). Here, we identify a new regulatory mechanism of forgetting whereby an AMPA-type glutamate receptor and a conserved serotonin receptor modulate the rate of forgetting in an antagonistic manner by acting in a pair of interneurons that plays a critical role in both learning and forgetting. In the mammalian brain, the membrane localization of AMPA-type ionotropic glutamate receptors encodes synaptic plasticity and memories (*33–35*). Meanwhile, AMPA receptors are also known to mediate cellular plasticity through several other mechanisms, including activity-dependent G protein–mediated regulation of channel activity and gene expression (*60, 61*). Here, we show that a worm AMPA receptor subunit GLR-1, which is homologous to GluA1 and GluA2 (*31*), acts in the interneuron RIA to inhibit forgetting, and SER-1, the worm homolog of the serotonin receptor HTR2B, acts in RIA to promote forgetting. In *C. elegans*, serotonin regulates complex behaviors that depend on the integrated function of multiple neurons expressing different serotonin receptors (*12, 14, 41–46, 62–64*). In the vertebrate brain, serotonin regulates emotion and cognitive functions, including learning and memory (*39, 40, 65*). HTR2B, the mammalian homolog of SER-1, is widely expressed in the brain (*66, 67*), and mutations in HTR2B are implicated in the pathology of psychotic disorders and defects in social and learning behaviors (*68, 69*). While GLR-1 is enriched in the proximal region of the RIA axon, SER-1 is enriched in the distal region of the axon (*37, 47*). Previous studies have shown that SER-1/HTR2B regulates neuronal functions by acting through an α subunit of G proteins, G_q (*62, 70*). We speculate that GLR-1 and SER-1 may regulate forgetting by, directly or indirectly, regulating G protein–mediated downstream pathways in an antagonistic manner. Our findings highlight the interaction of glutamatergic signaling and serotonergic signaling in orchestrating the function of neural circuits underlying complex behaviors.

MATERIALS AND METHODS
Experimental design
C. elegans hermaphrodite adult animals are used in this study, which are cultivated and maintained under standard conditions at 20°C (*71*). The behavioral assays used in this study—aversive olfactory training (*11, 14*), olfactory steering assay (*14*), and droplet assay (*11, 15*)—were previously described. Experiment design for calcium imaging was previously described (*14, 16*).

Strains and maintenance
The strains used in this study include the following: N2 (Bristol) (Figs. 1, 2, and 5 to 7and figs. S1, S2, and S5), JAC126 *csbIs4[Prgef-1::eGFP(+intron)::rpl-1(spliced)::unc-54 3′ UTR + lin-15]* (Fig. 4 and

fig. S4), ZC1508 *yxIs19[Pglr-3::GCaMP3.3, Punc-122::dsRed]* (Figs. 3 and 5 to 7), ZC2680 *yxEx1378[Pttx-3::GCaMP6, Punc-122::dsRed]* (Fig. 3), ZC2897 *yxEx1503[Pglr-3::HisCl1, Punc-122::gfp]* (Fig. 5 and fig. S6), DA1814 *ser-1(ok345)X* (Fig. 6 and figs. S5 and S7), ZC3109 *ser-1(ok345)X; yxIs19* (Fig. 6), ZC3238 *ser-1(ok345)X; yxIs19; yxEx1645[Pglr-3::ser-1cDNA::mCherry, Punc-122::gfp]* (Fig. 6), KP4 *glr-1(n2461)III* (Fig. 5 and fig. S5), ZC3135 *glr-1(n2461)III; yxIs19* (Fig. 5), ZC3136 *glr-1(n2461)III; wyIs93[Pglr-3::glr-1::gfp; Pglr-3::mCherry::rab-3; Punc-122::rfp]* (Fig. 5), ZC3149 *glr-1(n2461)III; ser-1(ok345)X* (Fig. 7), ZC3185 *glr-1(n2461)III; ser-1(ok345)X; yxIs19* (Fig. 7), *wyIs605[Pglr-3::ser-1::gfp; Pglr-3::tdTomato; Punc-122::rfp]* (Fig. 7), ZC3282 *glr-1(n2461)III; wyIs605* (Fig. 7), and ZC3394 *glr-1(n2461)III; yxIs19; yxEx1762[Pglr-3::glr-1cDNA, Punc-122::gfp]* (Fig. 5).

Generation of transgenes and transgenic animals
Gibson assembly (NEB) was used to generate *Pglr-3::ser-1(cDNA)::mCherry* by first digesting a plasmid containing *Pglr-3* (*14*) with NheI and KpnI and ligated with a *ser-1*cDNA generated by polymerase chain reaction (PCR) with primers 5′CATTTTCAGGAGGACCCTTGGCTAGCATGGGAATCTACCATTTCAAC3′ and 5′AGCTCAGATATCAATACCATGGTACCTTACAAGAATGTTTCCTTGATG3′. The resulting plasmid was used to generate a linear vector containing *Pglr-3::ser-1(cDNA)* with primers 5′GGCGGCATGGACGAGCTGTACAAGTAAGGTACCATGGTATTGATATCTGAGCTC3′ and 5′CTCGAGCATTTTTTCTACCGGTACCCTCAAGAATGTTTCCTTGATGGCACTATC3′.

An *mCherry* sequence was generated by PCR with primers 5′GATAGTGCCATCAAGGAAACATTCTTGAGGGTACCGGTAGAAAAAATGCTCGAG3′ and 5′GAGCTCAGATATCAATACCATGGTACCTTACTTGTACAGCTCGTCCATGCCGCC3′. Last, the *mCherry* fragment was assembled into the *Pglr-3::ser-1(cDNA)* linear vector to generate *Pglr-3::ser-1(cDNA)::mCherry*. *Pglr-3::HisCl1* was generated by an LR reaction (Invitrogen) of an entry vector containing *Pglr-3* (*14*) and a destination vector containing HisCl1 (*38*). To generate *Pglr-3::glr-1cDNA*, a *glr-1* cDNA fragment was generated by PCR from a cDNA library with primers 5′CATTTTCAGGAGGACCCTTGGCTAGCATGTTTTCTTCGTTTTCTTTTTTG3′ and 5′CTCAGATATCAATACCATGGTACCTCAGACAGCTGTGTTGTAGAGAG3′ and inserted into a destination vector to generate pDEST::*glr-1cDNA*, which was recombined with an entry vector containing *Pglr-3* through an LR reaction. The transgenes were injected at 20 to 30 ng/μl with *Punc-122::gfp* (10 ng/μl) as a coinjection marker as described (*72*).

Procedures for aversive training with pathogenic bacterium PA14 and forgetting
The aversive training with PA14 was performed similarly as previously described (*11, 14*). Briefly, *C. elegans* hermaphrodites were cultivated under standard conditions until the adult stage and then transferred to naive and training plates, which were prepared by respectively inoculating nematode growth medium [NGM; NaCl (3 g/liter), Bacto Peptone (2.5 g/liter), 1 mM $CaCl_2$, 1 mM $MgSO_4$, 25 mM KPO_4 (pH 6.0), 1.6% agar, and cholesterol (5 mg/liter)] plates with overnight Luria-Bertani (LB) culture of *E. coli* OP50 or *P. aeruginosa* PA14 and incubating at 26°C for 2 days. After training for 4 hours, animals on naive or training plates were analyzed individually for their olfactory responses to PA14 odorants using either single-worm chemotaxis assay or droplet olfactory assay. Some of the trained animals were transferred to previously prepared naive

plates to forget before their olfactory responses to PA14 odorants were analyzed. To control the time for training and forgetting, multiple plates of each treatment were set up when needed. The training time ranged from 4 hours to 4 hours and 25 min; the forgetting time ranged from 55 to 70 min.

Single-worm chemotactic steering assay

Chemotactic steering to PA14 odorants in single animals was performed and analyzed as previously described (14). A drop of 10 μl of 1.5 to 2 times diluted supernatant of an overnight culture of *P. aeruginosa* PA14 in NGM medium was placed in the center of a 10-cm NGM assay plate [NaCl (3 g/liter), 1 mM CaCl₂, 1 mM MgSO₄, 25 mM KPO₄ (pH 6.0), 1.6% agar, and cholesterol (5 mg/liter)] immediately before a worm was transferred to the plate at a position 1.5 cm away from the drop of PA14 culture supernatant. The tested worm crawled on an empty NGM plate for about 1 min to remove bacteria from its body before being transferred onto the plate for assay. The chemotactic movement of the worm was recorded using a Grasshopper3-GS3-U3-120S6M-C camera (FLIR Integrated Imaging Solutions) at 7 frames per second. The recording started after the worm was placed on the plate, and therefore, the worm may have traveled a little when the recording started. The recording stopped when a worm reached the culture supernatant. The recording stopped at 5 min after the start of the recording if a worm did not reach the culture supernatant within 5 min. Most of the worms completed the chemotaxis within 5 min. The recorded chemotactic steering was analyzed using a WormLab (MBF Bioscience) and a MATLAB (MathWorks) code (14) to generate navigation index and traveling distance between the starting point and the end point. The navigation index is defined as the ratio of radial speed (V_R) and the locomotory speed (V_L) (Fig. 1), and the navigation index of an assay is the mean of the navigation indexes calculated every 2 s. The total traveling distance is calculated using the position of the worm in each frame during steering. The learning index (LI) in fig. S5 is defined as Navigation Index_LI = (average naive navigation index – trained navigation index of tested animal)/(average naive navigation index + trained navigation index of tested animal) or Traveling distance_LI = (trained traveling distance of tested animal – average naive traveling distance)/(trained traveling distance of tested animal + average naive traveling distance). The average naive navigation index and average naive traveling distance are the average naive results tested on the same day.

Automated droplet olfactory assay

Olfactory preference for PA14 odorants was measured using an automated droplet assay as previously described (11, 15). Twelve droplets of 2-μl NGM buffer [NaCl (3 g/liter), 1 mM CaCl₂, 1 mM MgSO₄, and 25 mM KPO₄ (pH 6.0)] were placed on a sapphire window inside an airtight chamber that was connected by two airstreams odorized by going through an overnight NGM culture of *E. coli* OP50 or *P. aeruginosa* PA14. Worms were individually placed in the droplets and exposed to the odorants of OP50 or PA14 delivered to the chamber by the airstreams that alternated every 30 s. Locomotion of the worms was recorded, and the turning rate was analyzed by LabVIEW and MATLAB codes. When swimming, worms continuously thrash their bodies, which is occasionally disrupted by big body bends with a shape of the Greek letter Ω. Because Ω bends are followed by reorienting movements, such as reversals and turns, the rate of Ω bends inversely correlates with the preference of the worms for the tested odorant and is thus used to measure odorant preference. The preference between PA14 odorants and OP50 odorants was calculated using turning rate, and a learning index = average preference of naive animals (tested on the same day) – preference of a tested animal. A positive learning index indicates learned avoidance of PA14 odorants (11, 14, 15).

TRAP combined with RNA sequencing

TRAP combined with RNA sequencing was performed similarly as previously described (21). JAC126 animals that expressed an enhanced GFP (eGFP)–tagged ribosomal protein large subunit RPL-1 in the nervous system were cultivated on 15-cm NGM plates under standard conditions until the adult stage and were transferred onto 15-cm naive control plates or training plates. After 4-hour training, naive animals and around half of the trained animals were collected and lysed, and the remaining half of the trained worms were washed with NGM buffer and transferred to new naive plates for 1 hour before being harvested to make a lysate for the forgetting condition. Three independent experiments were performed to generate three lysate samples for naive and forgetting conditions and two samples for training condition. Immunoprecipitation with anti-eGFP antibody [HtzGFP_04 (clone19F7) and HtzGFP_02 (clone 19C8, The Rockefeller University] was performed to obtain eGFP-tagged ribosomes, which were used to isolate the associated mRNAs using TRI Reagent (T9424, Sigma-Aldrich). The mRNA samples were quantified using reverse transcription PCR (210210, QIAGEN) and then reverse-transcribed to generate cDNA libraries using TruSeq RNA Library Kit (RS-122-2001, Illumina). The cDNA libraries were sequenced by Illumina HiSeq 2000. Eight libraries of three conditions were sequenced with each library being sequenced ranging from 18 to 70 million reads. The reads were mapped to the annotated transcripts of the *C. elegans* genome to obtain counts for all uniquely mapped reads. STAR (version 2.7.0e) was used to align the sequencing results with the reference genome (Caenorhabditis_elegans. WBcel235.98), and HTSeq (version 0.11.2) was used to count the number of mapped reads. DESeq2 was used to identify differentially expressed genes under three conditions. Genes with mean normalized counts above the cutoff defined by the independent filtering parameter of DESeq2 were used as a background gene set for KEGG enrichment analysis and GO term analysis using functional annotation tool in the DAVID Bioinformatics Resources 6.8 (23–25). The principal component analysis plot was generated using the edgeR package in R (73). Hierarchical clustering and Pearson correlation were generated using basic functions in R (version 4.0.2, www.R-project.org/). Gene expression level was measured as $\log_2(CPM + 2)$, logarithm transformation of TMM (trimmed mean of M-values)-normalized count per million reads with two prior counts for each gene before transformation to avoid infinite values. To generate heatmap and hierarchical clustering, logarithm-transformed expression values were converted to z scores for each gene on the basis of the distribution of expression across all samples.

Calcium imaging

Calcium imaging was performed similarly as described (14) using a microfluidic device controlled by an AutoMate Scientific ValveBank perfusion system (Berkeley, CA) and a polydimethylsiloxane chip (17) on a confocal Nikon Eclipse Ti-E inverted microscope using a 40× oil-immersion objective. A worm was placed in the chip inside a channel that matched the size of an adult hermaphrodite. The worm with its head exposed to the fluidic streams in the chip was

stimulated by 0.5-Hz pulses of PA14 odorants or OP50 odorants controlled by the perfusion system. GCaMP3 (*18*) or GCaMP6 (*74*) signals in the anterior part of the worm body was recorded using an ANDOR iXon Ultra EMCCD camera at 5 frames per second, analyzed using ImageJ and a customized MATLAB code (MathWorks) (*14*). The region of interest (ROI) that contained the axonal domains of RIA or AIY was tracked using ImageJ plugin Manual Tracking. The sensory-evoked GCaMP signal (ΔF) is the fluorescence intensity of ROI (F) subtracted by baseline fluorescence intensity for AIY (F_{base}, average fluorescence intensity of the 2-s recording before the onset of sensory stimulus) or subtracted by mean intensity of the bottom 5% fluorescence signals of each recording for RIA (F_{base}), i.e., $\Delta F = F - F_{base}$. Fourier transform was applied to the time series of $\Delta F/F_{base}$% for each animal to obtain the amplitude of 0.5-Hz peak. Multiple worms were recorded and analyzed for each experiment.

Confocal microscopy

Fluorescence signals generated by *Pglr-3::glr-1::GFP*, *Pglr-3::ser-1::GFP*, or *Pglr-3::tdTomato* were recorded by collecting *Z*-stack images using a confocal Nikon Eclipse Ti-E inverted microscope with a 40× oil-immersion objective and an ANDOR iXon Ultra EMCCD camera. Intensity of GLR-1::GFP, SER-1::GFP, or tdTomato in RIA axon was measured from an ROI containing an axonal region in maximal intensity projection of the *Z*-stack images of each worm using ImageJ. Background fluorescence intensity was subtracted using the signal from a background area of the same shape and size. The polarity index = (fluorescence intensity of a distal region of RIA axon)/(fluorescence intensity of a distal region of RIA axon + fluorescence intensity of a proximal region of RIA axon), similar to previously described (*37*). Multiple worms were recorded and analyzed.

Statistical analysis

Statistical tests were performed using GraphPad Prism (version 9.0.0). The tests used in each experiment, values of *n* numbers, statistical significance (*P* values), and other related measures are reported in the legends of each figure and supplementary figure and listed in data S6. Asterisks denote significant difference (****$P < 0.0001$, ***$P < 0.001$, **$P < 0.01$, and *$P < 0.05$).

SUPPLEMENTARY MATERIALS

Supplementary material for this article is available at https://science.org/doi/10.1126/sciadv.abi9071

View/request a protocol for this paper from *Bio-protocol*.

REFERENCES AND NOTES

1. N. E. Spear, Retrieval of memory in animals. *Psychol. Rev.* **80**, 163–194 (1973).
2. J. T. Wixted, The psychology and neuroscience of forgetting. *Annu. Rev. Psychol.* **55**, 235–269 (2004).
3. R. L. Davis, Y. Zhong, The biology of forgetting–A perspective. *Neuron* **95**, 490–503 (2017).
4. L. de Hoz, S. J. Martin, R. G. Morris, Forgetting, reminding, and remembering: The retrieval of lost spatial memory. *PLOS Biol.* **2**, e225 (2004).
5. B. Deweer, S. J. Sara, Background stimuli as a reminder after spontaneous forgetting: Role of duration of cuing and cuing-test interval. *Anim. Learn. Behav.* **12**, 238–247 (1984).
6. D. T. Feldman, W. C. Gordon, The alleviation of short-term retention decrements with reactivation. *Learn. Motiv.* **10**, 198–210 (1979).
7. R. Silvestri, M. Rohrbaugh, D. C. Riccio, Conditions influencing the retention of learned fear in young rats. *Dev. Psychol.* **2**, 389–395 (1970).
8. M. Costanzi, B. Cianfanelli, A. Santirocchi, S. Lasaponara, P. Spataro, C. Rossi-Arnaud, V. Cestari, Forgetting unwanted memories: Active forgetting and implications for the development of psychological disorders. *J. Pers. Med.* **11**, 241 (2021).
9. T. Dong, J. He, S. Wang, L. Wang, Y. Cheng, Y. Zhong, Inability to activate Rac1-dependent forgetting contributes to behavioral inflexibility in mutants of multiple autism-risk genes. *Proc. Natl. Acad. Sci. U.S.A.* **113**, 7644–7649 (2016).
10. M. W. Tan, S. Mahajan-Miklos, F. M. Ausubel, Killing of *Caenorhabditis elegans* by *Pseudomonas aeruginosa* used to model mammalian bacterial pathogenesis. *Proc. Natl. Acad. Sci. U.S.A.* **96**, 715–720 (1999).
11. H. I. Ha, M. Hendricks, Y. Shen, C. V. Gabel, C. Fang-Yen, Y. Qin, D. Colón-Ramos, K. Shen, A. D. T. Samuel, Y. Zhang, Functional organization of a neural network for aversive olfactory learning in *Caenorhabditis elegans*. *Neuron* **68**, 1173–1186 (2010).
12. X. Jin, N. Pokala, C. I. Bargmann, Distinct circuits for the formation and retrieval of an imprinted olfactory memory. *Cell* **164**, 632–643 (2016).
13. Y. Iino, K. Yoshida, Parallel use of two behavioral mechanisms for chemotaxis in *Caenorhabditis elegans*. *J. Neurosci.* **29**, 5370–5380 (2009).
14. H. Liu, W. Yang, T. Wu, F. Duan, E. Soucy, Y. Zhang, Cholinergic sensorimotor integration regulates olfactory steering. *Neuron* **97**, 390–405.e3 (2018).
15. L. Luo, C. V. Gabel, H. I. Ha, Y. Zhang, A. D. Samuel, Olfactory behavior of swimming *C. elegans* analyzed by measuring motile responses to temporal variations of odorants. *J. Neurophysiol.* **99**, 2617–2625 (2008).
16. M. Hendricks, H. Ha, N. Maffey, Y. Zhang, Compartmentalized calcium dynamics in a *C. elegans* interneuron encode head movement. *Nature* **487**, 99–103 (2012).
17. N. Chronis, M. Zimmer, C. I. Bargmann, Microfluidics for in vivo imaging of neuronal and behavioral activity in *Caenorhabditis elegans*. *Nat. Methods* **4**, 727–731 (2007).
18. L. Tian, S. A. Hires, T. Mao, D. Huber, M. E. Chiappe, S. H. Chalasani, L. Petreanu, J. Akerboom, S. A. McKinney, E. R. Schreiter, C. I. Bargmann, V. Jayaraman, K. Svoboda, L. L. Looger, Imaging neural activity in worms, flies and mice with improved GCaMP calcium indicators. *Nat. Methods* **6**, 875–881 (2009).
19. J. G. White, E. Southgate, J. N. Thomson, S. Brenner, The structure of the nervous system of the nematode *Caenorhabditis elegans*. *Philos. Trans. R. Soc. Lond. B Biol. Sci.* **314**, 1–340 (1986).
20. M. Heiman, A. Schaefer, S. Gong, J. D. Peterson, M. Day, K. E. Ramsey, M. Suárez-Fariñas, C. Schwarz, D. A. Stephan, D. J. Surmeier, P. Greengard, N. Heintz, A translational profiling approach for the molecular characterization of CNS cell types. *Cell* **135**, 738–748 (2008).
21. X. Gracida, J. A. Calarco, Cell type-specific transcriptome profiling in *C. elegans* using the translating ribosome affinity purification technique. *Methods* **126**, 130–137 (2017).
22. E. R. Troemel, S. W. Chu, V. Reinke, S. S. Lee, F. M. Ausubel, D. H. Kim, p38 MAPK regulates expression of immune response genes and contributes to longevity in *C. elegans*. *PLoS Genet* **2**, e183 (2006).
23. D. W. Huang, B. T. Sherman, R. A. Lempicki, Systematic and integrative analysis of large gene lists using DAVID bioinformatics resources. *Nat Protoc* **4**, 44–57 (2009).
24. D. W. Huang, B. T. Sherman, R. A. Lempicki, Bioinformatics enrichment tools: Paths toward the comprehensive functional analysis of large gene lists. *Nucleic Acids Res* **37**, 1–13 (2009).
25. M. Kanehisa, S. Goto, KEGG: Kyoto Encyclopedia of Genes and Genomes. *Nucleic Acids Res.* **28**, 27–30 (2000).
26. O. Hobert, The neuronal genome of *Caenorhabditis elegans*. *WormBook* **2013**, 1–106 (2013).
27. R. Dringen, Metabolism and functions of glutathione in brain. *Prog. Neurobiol.* **62**, 649–671 (2000).
28. T. W. Sedlak, B. D. Paul, G. M. Parker, L. D. Hester, A. M. Snowman, Y. Taniguchi, A. Kamiya, S. H. Snyder, A. Sawa, The glutathione cycle shapes synaptic glutamate activity. *Proc. Natl. Acad. Sci. U.S.A.* **116**, 2701–2706 (2019).
29. M. Koga, A. V. Serritella, M. M. Messmer, A. Hayashi-Takagi, L. D. Hester, S. H. Snyder, A. Sawa, T. W. Sedlak, Glutathione is a physiologic reservoir of neuronal glutamate. *Biochem. Biophys. Res. Commun.* **409**, 596–602 (2011).
30. G. D. Ferguson, W. J. Bridge, The glutathione system and the related thiol network in *Caenorhabditis elegans*. *Redox Biol.* **24**, 101171 (2019).
31. P. J. Brockie, D. M. Madsen, Y. Zheng, J. Mellem, A. V. Maricq, Differential expression of glutamate receptor subunits in the nervous system of *Caenorhabditis elegans* and their regulation by the homeodomain protein UNC-42. *J. Neurosci.* **21**, 1510–1522 (2001).
32. S. R. Taylor, G. Santpere, A. Weinreb, A. Barrett, M. B. Reilly, C. Xu, E. Varol, P. Oikonomou, L. Glenwinkel, R. M. Whirter, A. Poff, M. Basavaraju, I. Rafi, E. Yemini, S. J. Cook, A. Abrams, B. Vidal, C. Cros, S. Tavazoie, N. Sestan, M. Hammarlund, O. Hobert, D. M. Miller III, Molecular topography of an entire nervous system. *Cell* **184**, 4329–4347.e23 (2021).
33. A. Awasthi, B. Ramachandran, S. Ahmed, E. Benito, Y. Shinoda, N. Nitzan, A. Heukamp, S. Rannio, H. Martens, J. Barth, K. Burk, Y. T. Wang, A. Fischer, C. Dean, Synaptotagmin-3 drives AMPA receptor endocytosis, depression of synapse strength, and forgetting. *Science* **363**, eaav1483 (2019).
34. J. M. Henley, K. A. Wilkinson, Synaptic AMPA receptor composition in development, plasticity and disease. *Nat. Rev. Neurosci.* **17**, 337–350 (2016).

35. J. D. Shepherd, R. L. Huganir, The cell biology of synaptic plasticity: AMPA receptor trafficking. *Annu. Rev. Cell Dev. Biol.* **23**, 613–643 (2007).

36. M. K. Choi, H. Liu, T. Wu, W. Yang, Y. Zhang, NMDAR-mediated modulation of gap junction circuit regulates olfactory learning in *C. elegans*. *Nat. Commun.* **11**, 3467 (2020).

37. M. A. Margeta, G. J. Wang, K. Shen, Clathrin adaptor AP-1 complex excludes multiple postsynaptic receptors from axons in *C. elegans*. *Proc. Natl. Acad. Sci. U.S.A.* **106**, 1632–1637 (2009).

38. N. Pokala, Q. Liu, A. Gordus, C. I. Bargmann, Inducible and titratable silencing of *Caenorhabditis elegans* neurons in vivo with histamine-gated chloride channels. *Proc. Natl. Acad. Sci. U.S.A.* **111**, 2770–2775 (2014).

39. K. Iigaya, M. S. Fonseca, M. Murakami, Z. F. Mainen, P. Dayan, An effect of serotonergic stimulation on learning rates for rewards apparent after long intertrial intervals. *Nat. Commun.* **9**, 2477 (2018).

40. C. M. Teixeira, Z. B. Rosen, D. Suri, Q. Sun, M. Hersh, D. Sargin, I. Dincheva, A. A. Morgan, S. Spivack, A. C. Krok, T. Hirschfeld-Stoler, E. K. Lambe, S. A. Siegelbaum, M. S. Ansorge, Hippocampal 5-HT input regulates memory formation and schaffer collateral excitation. *Neuron* **98**, 992–1004.e4 (2018).

41. Y. Zhang, H. Lu, C. I. Bargmann, Pathogenic bacteria induce aversive olfactory learning in Caenorhabditis elegans. *Nature* **438**, 179–184 (2005).

42. J. Morud, I. Hardege, H. Liu, T. Wu, M. K. Choi, S. Basu, Y. Zhang, W. R. Schafer, Deorphanization of novel biogenic amine-gated ion channels identifies a new serotonin receptor for learning. *Curr. Biol.* **31**, 4282–4292.e6 (2021).

43. L. Carnell, J. Illi, S. W. Hong, S. L. McIntire, The G-protein-coupled serotonin receptor SER-1 regulates egg laying and male mating behaviors in *Caenorhabditis elegans*. *J. Neurosci.* **25**, 10671–10681 (2005).

44. S. Dernovici, T. Starc, J. A. Dent, P. Ribeiro, The serotonin receptor SER-1 (5HT2ce) contributes to the regulation of locomotion in *Caenorhabditis elegans*. *Dev. Neurobiol.* **67**, 189–204 (2007).

45. M. Guo, M. Ge, M. A. Berberoglu, J. Zhou, L. Ma, J. Yang, Q. Dong, Y. Feng, Z. Wu, Z. Dong, Dissecting molecular and circuit mechanisms for inhibition and delayed response of ASI neurons during nociceptive stimulus. *Cell Rep* **25**, 1885–1897.e9 (2018).

46. G. P. Harris, V. M. Hapiak, R. T. Wragg, S. B. Miller, L. J. Hughes, R. J. Hobson, R. Steven, B. Bamber, R. W. Komuniecki, Three distinct amine receptors operating at different levels within the locomotory circuit are each essential for the serotonergic modulation of chemosensation in *Caenorhabditis elegans*. *J. Neurosci.* **29**, 1446–1456 (2009).

47. P. Li, S. A. Merrill, E. M. Jorgensen, K. Shen, Two clathrin adaptor protein complexes instruct axon-dendrite polarity. *Neuron* **90**, 564–580 (2016).

48. R. Ranganathan, S. C. Cannon, H. R. Horvitz, MOD-1 is a serotonin-gated chloride channel that modulates locomotory behaviour in *C. elegans*. *Nature* **408**, 470–475 (2000).

49. Z. Chen, M. Hendricks, A. Cornils, W. Maier, J. Alcedo, Y. Zhang, Two insulin-like peptides antagonistically regulate aversive olfactory learning in *C. elegans*. *Neuron* **77**, 572–585 (2013).

50. T. Wu, F. Duan, W. Yang, H. Liu, A. Caballero, D. A. F. de Abreu, A. R. Dar, J. Alcedo, Q. Ch'ng, R. A. Bucher, Y. Zhang, Pheromones modulate learning by regulating the balanced signals of two insulin-like peptides. *Neuron* **104**, 1095–1109.e5 (2019).

51. X. Zhang, Y. Zhang, DBL-1, a TGF-β, is essential for *Caenorhabditis elegans* aversive olfactory learning. *Proc. Natl. Acad. Sci. U.S.A.* **109**, 17081–17086 (2012).

52. A. Zaslaver, I. Liani, O. Shtangel, S. Ginzburg, L. Yee, P. W. Sternberg, Hierarchical sparse coding in the sensory system of *Caenorhabditis elegans*. *Proc. Natl. Acad. Sci. U.S.A.* **112**, 1185–1189 (2015).

53. Y. Qin, X. Zhang, Y. Zhang, A neuronal signaling pathway of CaMKII and Gqα regulates experience-dependent transcription of tph-1. *J. Neurosci.* **33**, 925–935 (2013).

54. J. L. Rhoades, J. C. Nelson, I. Nwabudike, S. K. Yu, I. G. McLachlan, G. K. Madan, E. Abebe, J. R. Powers, D. A. Colon-Ramos, S. W. Flavell, ASICs mediate food responses in an enteric serotonergic neuron that controls foraging behaviors. *Cell* **176**, 85–97.e14 (2019).

55. E. Serrano-Saiz, R. J. Poole, T. Felton, F. Zhang, E. D. De La Cruz, O. Hobert, Modular control of glutamatergic neuronal identity in *C. elegans* by distinct homeodomain proteins. *Cell* **155**, 659–673 (2013).

56. N. Hadziselimovic, V. Vukojevic, F. Peter, A. Milnik, M. Fastenrath, B. G. Fenyves, P. Hieber, P. Demougin, C. Vogler, D. J. F. de Quervain, A. Papassotiropoulos, A. Stetak, Forgetting is regulated via Musashi-mediated translational control of the Arp2/3 complex. *Cell* **156**, 1153–1166 (2014).

57. A. Inoue, E. Sawatari, N. Hisamoto, T. Kitazon, T. Teramoto, M. Fujiwara, K. Matsumoto, T. Ishihara, Forgetting in *C. elegans* is accelerated by neuronal communication via the TIR-1/JNK-1 pathway. *Cell Rep* **3**, 808–819 (2013).

58. Y. Shuai, B. Lu, Y. Hu, L. Wang, K. Sun, Y. Zhong, Forgetting is regulated through Rac activity in Drosophila. *Cell* **140**, 579–589 (2010).

59. J. M. Sabandal, J. A. Berry, R. L. Davis, Dopamine-based mechanism for transient forgetting. *Nature* **591**, 426–430 (2021).

60. V. R. Rao, S. A. Pintchovski, J. Chin, C. L. Peebles, S. Mitra, S. Finkbeiner, AMPA receptors regulate transcription of the plasticity-related immediate-early gene Arc. *Nat. Neurosci.* **9**, 887–895 (2006).

61. F. Kawai, P. Sterling, AMPA receptor activates a G-protein that suppresses a cGMP-gated current. *J. Neurosci.* **19**, 2954–2959 (1999).

62. C. M. Dempsey, S. M. Mackenzie, A. Gargus, G. Blanco, J. Y. Sze, Serotonin (5HT), fluoxetine, imipramine and dopamine target distinct 5HT receptor signaling to modulate Caenorhabditis elegans egg-laying behavior. *Genetics* **169**, 1425–1436 (2005).

63. R. J. Hobson, V. M. Hapiak, H. Xiao, K. L. Buehrer, P. R. Komuniecki, R. W. Komuniecki, SER-7, a *Caenorhabditis elegans* 5-HT7-like receptor, is essential for the 5-HT stimulation of pharyngeal pumping and egg laying. *Genetics* **172**, 159–169 (2006).

64. G. A. Lemieux, K. A. Cunningham, L. Lin, F. Mayer, Z. Werb, K. Ashrafi, Kynurenic acid is a nutritional cue that enables behavioral plasticity. *Cell* **160**, 119–131 (2015).

65. I. Lucki, The spectrum of behaviors influenced by serotonin. *Biol. Psychiatry* **44**, 151–162 (1998).

66. D. S. Choi, L. Maroteaux, Immunohistochemical localisation of the serotonin 5-HT2B receptor in mouse gut, cardiovascular system, and brain. *FEBS Lett.* **391**, 45–51 (1996).

67. M. S. Duxon, T. P. Flanigan, A. C. Reavley, G. S. Baxter, T. P. Blackburn, K. C. F. Fone, Evidence for expression of the 5-hydroxytryptamine-2B receptor protein in the rat central nervous system. *Neuroscience* **76**, 323–329 (1997).

68. L. Bevilacqua, S. Doly, J. Kaprio, Q. Yuan, R. Tikkanen, T. Paunio, Z. Zhou, J. Wedenoja, L. Maroteaux, S. Diaz, A. Belmer, C. A. Hodgkinson, L. Dell'Osso, J. Suvisaari, E. Coccaro, R. J. Rose, L. Peltonen, M. Virkkunen, D. Goldman, A population-specific HTR2B stop codon predisposes to severe impulsivity. *Nature* **468**, 1061–1066 (2010).

69. P. M. Pitychoutis, A. Belmer, I. Moutkine, J. Adrien, L. Maroteaux, Mice lacking the serotonin Htr2B receptor gene present an antipsychotic-sensitive schizophrenic-like phenotype. *Neuropsychopharmacology* **40**, 2764–2773 (2015).

70. L. Maroteaux, E. Ayme-Dietrich, G. Aubertin-Kirch, S. Banas, E. Quentin, R. Lawson, L. Monassier, New therapeutic opportunities for 5-HT2 receptor ligands. *Pharmacol. Ther.* **170**, 14–36 (2017).

71. S. Brenner, The genetics of *Caenorhabditis elegans*. *Genetics* **77**, 71–94 (1974).

72. C. C. Mello, J. M. Kramer, D. Stinchcomb, V. Ambros, Efficient gene transfer in *C.elegans*: Extrachromosomal maintenance and integration of transforming sequences. *EMBO J* **10**, 3959–3970 (1991).

73. M. D. Robinson, D. J. McCarthy, G. K. Smyth, edgeR: A Bioconductor package for differential expression analysis of digital gene expression data. *Bioinformatics* **26**, 139–140 (2010).

74. T. W. Chen, T. J. Wardill, Y. Sun, S. R. Pulver, S. L. Renninger, A. Baohan, E. R. Schreiter, R. A. Kerr, M. B. Orger, V. Jayaraman, L. L. Looger, K. Svoboda, D. S. Kim, Ultrasensitive fluorescent proteins for imaging neuronal activity. *Nature* **499**, 295–300 (2013).

Science Advances

Forgetting generates a novel state that is reactivatable

He LiuTaihong WuXicotencatl Gracida CanalesMin WuMyung-Kyu ChoiFengyun DuanJohn A. CalarcoYun Zhang

View the article online
https://www.science.org/doi/10.1126/sciadv.abi9071
Permissions
https://www.science.org/help/reprints-and-permissions

Use of this article is subject to the Terms of service